

High efficiency Silicon-on-Insulator grating coupler based on a poly-Silicon overlay

Günther Roelkens, Dries Van Thourhout, Roel Baets

Photonics Research Group, Ghent University – IMEC, Sint-Pietersnieuwstraat 41, B-9000 Ghent, Belgium

Gunter.Roelkens@intec.Ugent.be

Abstract: A high efficiency broadband grating coupler for Silicon-On-Insulator waveguides was designed. The grating coupler is defined by locally adding a poly-Silicon layer on top of the existing waveguide layer structure prior to grating etching. Adding this poly-Silicon layer reshapes the grating structure which changes its diffraction properties. Coupling efficiencies as high as 78% at a wavelength of 1.55 μm are calculated and the optical 3dB bandwidth of the device is about 85nm. The device layout is compatible with standard CMOS technology processing.

©2006 Optical Society of America

OCIS codes: (130.0130) Integrated optics; (050.2770) Gratings

References and Links

1. W. Bogaerts, R. Baets, P. Dumon, V. Wiaux, S. Beckx, D. Taillaert, B. Luyssaert, J. Van Campenhout, P. Bienstman and D. Van Thourhout, "Nanophotonic waveguides in Silicon-on-Insulator fabricated with CMOS technology," *J. Lightwave Technol.* **23**, 401-412 (2005).
2. A. Sure, T. Dillon, J. Murakowski, C.C. Lin, D. Pustai and D.W. Prather, "Fabrication and characterization of three-dimensional silicon tapers," *Opt. Express* **11**, 3555-3561 (2003).
3. T. Shoji, T. Tsuchizawa, T. Watanabe, K. Yamada and H. Morita, "Low loss mode size converter from 0.3 μm square Si waveguides to single mode fibers," *Electron. Lett.* **38**, 1669-1670 (2002).
4. D. Taillaert, W. Bogaerts, P. Bienstman, T. F. Krauss, P. Van Daele, I. Moerman, S. Verstuyft, K. De Mesel and R. Baets, "An out-of-plane grating coupler for efficient butt-coupling between compact planar waveguides and single mode fibers," *J. Quantum Electron.* **38**, 949-956 (2002).
5. D. Taillaert, H. Chong, P. I. Borel, L. H. Frandsen, R. M. De La Rue and R. Baets, "A compact two-dimensional grating coupler used as a polarization splitter," *Photon. Technol. Lett.* **15**, 1249-1252 (2003).
6. D. Taillaert, F. Van Laere, M. Ayre, W. Bogaerts, D. Van Thourhout, P. Bienstman and R. Baets, "Grating couplers for coupling between optical fibers and nanophotonic waveguides," *Jap. J. Appl. Phys.* **45**, 6071-6077 (2006).
7. F. Van Laere, G. Roelkens, J. Schrauwen, D. Taillaert, P. Dumon, W. Bogaerts, D. Van Thourhout and R. Baets, "Compact grating couplers between optical fibers and Silicon-on-Insulator photonic wire waveguides with 69% coupling efficiency," conference on Optical Fiber Communication PDP15 (2006).
8. D. Taillaert, P. Bienstman and R. Baets, "Compact efficient broadband grating coupler for Silicon-on-Insulator waveguides," *Opt. Lett.* **29**, 2749-2752 (2004).
9. B. Wang, J. H. Jiang and G. P. Nordin, "Embedded slanted grating for vertical coupling between fibers and Silicon-on-Insulator planar waveguides," *Photon. Technol. Lett.* **17**, 1884-1887 (2005).
10. P. Bienstman and R. Baets, "Rigorous and efficient optical VCSEL model based on vectorial eigenmode expansion and perfectly matched layers," *IEE Proc.-J:Optoelectron.* **149**, 161-169 (2002).

1. Introduction

Silicon-on-Insulator is emerging as an interesting platform for integrated optics due to the high index contrast between the silicon core and the oxide cladding ($\Delta n \approx 2$). This enables large density integrated optical circuits, which can be fabricated by standard CMOS technology [1]. One of the drawbacks of the high index contrast is the large mismatch in mode size and shape between the fundamental mode of the SOI waveguide and the mode of the optical fiber making efficient coupling of light from fiber to waveguide an important issue. Several approaches are being envisaged in literature to overcome this problem. 3D taper structures can adiabatically transform the fiber waveguide mode to the mode of an SOI waveguide [2]. However, the definition of the taper requires gray scale lithography, which is difficult to

control. An inverted taper approach uses only planar waveguide definition technology to make an adiabatic taper structure, however this type of devices requires a lensed or high numerical aperture fiber with reduced core size to obtain efficient coupling over a reasonable device length [3]. As proposed in literature, one dimensional [4] or two dimensional [5] grating structures can also be used to couple light from a fiber into an SOI waveguide. These grating couplers have the advantage of not requiring polished facets for coupling, which enables wafer scale testing of the integrated circuits. Devices are very compact and have a large optical bandwidth. Although one dimensional grating couplers are very polarization dependent, a polarization diversity scheme based on a two dimensional grating coupler can be used in practical applications [5]. The reported fiber coupling efficiency obtained with standard uniform grating structures is limited. In Ref. [5] 20% fiber coupling efficiency was experimentally obtained for a two dimensional grating coupler. In Ref. [6], a one dimensional grating structure with a theoretical coupling efficiency of 37% was designed, while experimentally 31% coupling efficiency was obtained. This moderate coupling efficiency is inherent to the device structure due to the substantial fraction of incident power that is diffracted towards the Silicon substrate and the mismatch in the field profile between the upwards diffracted light and the Gaussian fiber mode. In order to increase the efficiency of the grating coupler structure, different strategies can be followed. One strategy is to include a bottom mirror to redirect the downwards diffracted light. This can be a gold bottom mirror [7] or a DBR-type mirror [8]. A second strategy is to optimize the dimensions of the individual grating periods to match the profile of the diffracted light with that of the fiber mode [8], while in a third strategy slanted gratings are used to optimize the coupling efficiency [9]. Although high efficiencies can be obtained, the technology required for fabrication is not CMOS compatible or is very complex. Therefore, we present here a way to increase the coupling efficiency by simply adding an additional layer of poly-Silicon before grating definition. This additional poly-Silicon layer reshapes the grating structure which changes its diffraction properties to improve the fiber coupling efficiency.

2. Proposed device layout

The structure we propose is depicted in Fig. 1. It consist of an SOI waveguide structure with a crystalline Silicon waveguide layer of 220nm thick and a buried oxide layer of 2 μ m in order to prevent leakage of light to the Silicon substrate. Locally, an additional poly-crystalline silicon layer is deposited, in which the grating coupler is etched (possibly extending the etch into the crystalline Silicon layer). The optical fiber is slightly tilted with respect to the vertical axis in order to prevent a large second order reflection and is assumed to be AR coated for a wavelength of 1.55 μ m. Reflections at the fiber facet can also be avoided by adding an index matching glue between the optical fiber and the grating coupler.

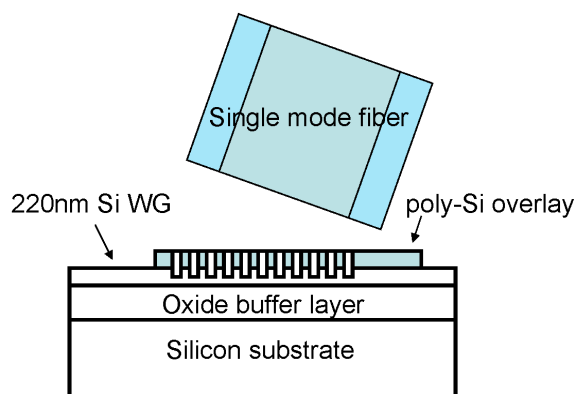


Fig. 1. Proposed device layout for high efficiency coupling to an optical fiber.

A possible processing scheme to define this type of grating structure is depicted in Fig. 2. Only standard CMOS processes are used, making this type of grating coupler applicable for mass manufacturing. The process sequence starts by depositing a SiO_2 hard mask on the SOI waveguide structure and opening a window in the hard mask for the definition of the poly-Silicon layer. After deposition of a thick poly-Silicon layer, a chemical mechanical polishing step is used to define the poly-Silicon overlay using the oxide mask as a polish stop layer. Finally, the grating is etched in the poly-Silicon layer and the oxide mask is removed.

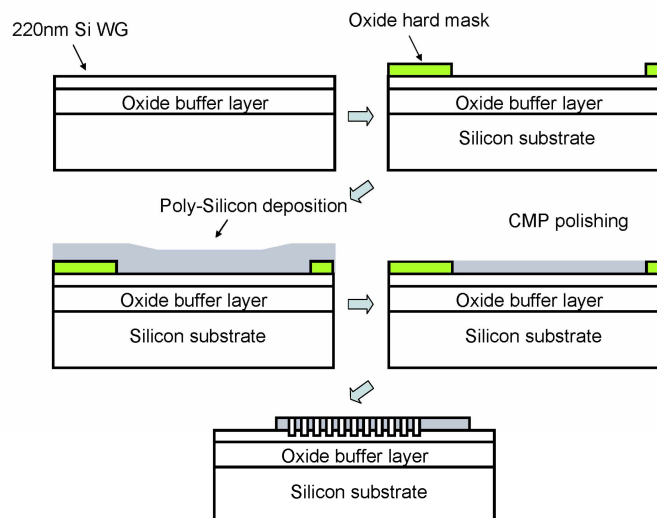


Fig. 2. CMOS compatible fabrication process for the poly-Silicon overlay grating couplers.

3. Device optimization

To optimize the structure, the influence of the thickness of the poly-Silicon layer, etch depth of the grating and grating period on the directionality of the grating (being the amount of power diffracted upwards for a 20 period long grating) was assessed. Simulations were performed using CAMFR [10], a two-dimensional fully vectorial solver based on eigenmode expansion. TE polarization and a wavelength of $1.55\mu\text{m}$ are assumed. As high index contrast

waveguide structures behave very differently for TE and TM polarization, only TE polarization is considered. However, two dimensional grating structures can be used to tackle these polarization issues [5] or the design of the one dimensional grating structure can be adapted to accommodate high coupling efficiency for TM polarization. The simulation results are plotted in Fig. 3 (for a grating duty cycle of 50%). Light is injected into the SOI waveguide and is scattered by the grating coupler. This figure shows that an optimal directionality of 85% is achieved for a poly-Silicon thickness of 150nm, an etch depth of 220nm and a grating period of 610nm.

Simulation shows that these parameters for the grating structure result in a 10 degree off vertical angle of light diffraction at 1.55 μ m (and hence a 10 degree tilt of the optical fiber for efficient coupling). In the case of a standard grating coupler structure with a 220nm Silicon waveguide layer (i.e. without the additional poly-Silicon layer), a separate optimization of the grating etch depth, grating period and buried oxide layer thickness results in an optimal grating directionality of 55%, significantly lower than the results obtained in Fig. 3. The field plot of a separately optimized grating coupler structure with and without the poly-Silicon overlay is shown in Fig. 4, from which the improvement in grating directionality is clear. While the buried oxide layer thickness plays an important role in the standard grating coupler design to achieve constructive interference between the reflected wave at the oxide-Silicon interface and the directly upwards radiated wave, this is far less the case in the optimized grating coupler structure, which inherently is more directional.

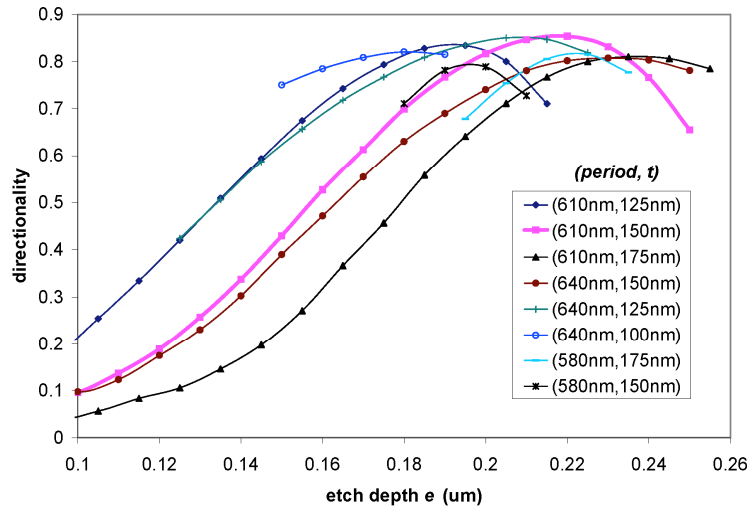


Fig. 3. Influence of the grating etch depth, poly-Silicon overlay thickness and grating period on the directionality of a uniform grating structure (grating duty cycle 50%).

To calculate the coupling efficiency to fiber, we assumed an optical fiber with a core diameter of 9 μ m and a refractive index contrast between core and cladding of 0.005. The grating coupling structure is excited by the power normalized fundamental Silicon waveguide mode and the diffracted field pattern in the air cladding is calculated. The coupling efficiency is then calculated by evaluating the overlap integral

$$\eta = \left| \int \mathbf{E} \times \mathbf{H}_{fib}^* \cdot d\mathbf{S} \right|^2 \quad (1)$$

in which \mathbf{E} is the electric field vector of the diffracted light in the air cladding and \mathbf{H}_{fib} is the magnetic field of the fiber waveguide mode, which is also normalized in power. $d\mathbf{S}$ lies along

the surface normal of an integration pad in the air cladding which spans the complete grating coupler structure length. This overlap integral is evaluated for different fiber positions along the direction of propagation of the excited Silicon waveguide mode resulting in the optimal fiber position and power coupling efficiency.

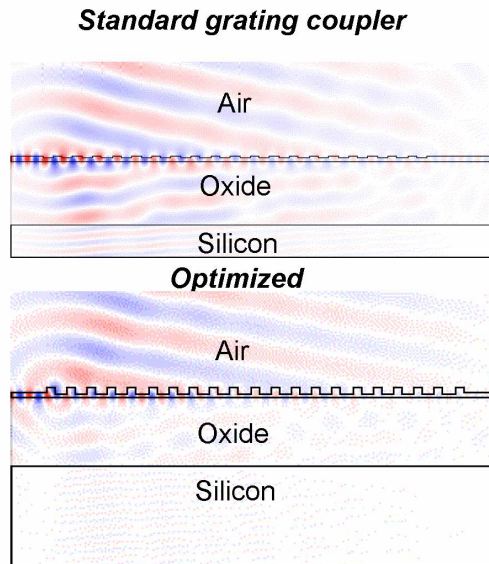


Fig. 4. Field plot comparison of the optimized standard grating coupler design and the optimized grating coupler structure using a poly-Silicon overlay.

For the case of a uniform grating with the parameters mentioned above (grating period 610nm, duty cycle 50%, poly-silicon overlay thickness 150nm and etch depth of 220nm) a coupling efficiency of 66% at 1.55 μ m is obtained for a fiber that is tilted 10 degrees with respect to the vertical axis.

The origin of the increased directionality of the grating is attributed to the increased vertical asymmetry in the grating structure. In the case of a vertically symmetric grating (by etching completely through the Silicon waveguide layer and applying the same top and bottom cladding materials) the diffraction pattern is identical in top and bottom cladding. The grating directionality is therefore limited to 50 percent. By reducing the etch depth of the grating, the asymmetry of the grating structure is increased (which can improve the directionality) at the expense of a longer coupling length of the grating as the strength of the grating is reduced. For a uniform grating, the diffracted field profile is exponentially decaying along the length of the grating structure and no perfect match with the Gaussian field profile of the optical fiber is achieved. An optimal grating coupler length exists for which the overlap between the exponentially decaying diffracted field and the Gaussian mode profile is maximal. As a high coupling efficiency grating structure has to be designed close to this optimal coupling length, this also determines the directionality of the grating. By adding the additional poly-Silicon layer an additional degree of freedom is introduced in the design of the structure, thereby allowing an optimization of both the directionality of the grating coupler and the coupling length of the grating. High directionality can be obtained due to the destructive interference of light diffracted towards the substrate while constructive interference is obtained for diffraction in the air cladding. This is an intrinsic property of the excited Bloch mode of the designed periodic grating structure as the directionality is nearly independent of the thickness of the buried oxide layer showing that the reflection at the buried

oxide / Silicon substrate interface does not significantly affect the constructive and destructive interference properties (as is the case in the standard grating coupler structure).

In order to further increase the fiber coupling efficiency, a non-uniform grating structure can be designed in order for the diffracted light to better match the Gaussian profile of the optical fiber. A genetic algorithm approach was used to optimize the width of the individual grating teeth and slits while keeping the etch depth constant. To be definable using CMOS deep UV lithography, the smallest feature size allowed in the genetic algorithm was set to 200nm. The evolution of the optimal coupling efficiency to fiber as a function of the genetic algorithm generation is shown in Fig. 5. An optimal fiber coupling efficiency of 78% was obtained.

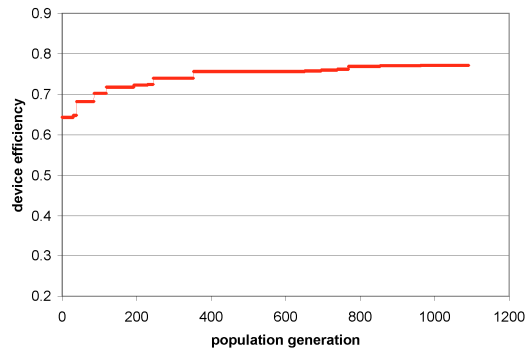


Fig. 5. Evolution of the device efficiency as a function of the genetic algorithm population generation.

The grating teeth and slit widths for which this high coupling efficiency was achieved are tabulated in Table 1. It turns out that a rather random varying local grating period and duty cycle shows to be optimal, which justifies the use of a genetic algorithm optimization approach.

Table 1. Optimal grating tooth and slit widths obtained from a genetic algorithm optimization

Period	Tooth width(nm)	Slit width(nm)	Period	Tooth width(nm)	Slit width(nm)
1	220nm	360nm	11	300nm	330nm
2	230nm	410nm	12	230nm	370nm
3	280nm	310nm	13	290nm	290nm
4	260nm	380nm	14	330nm	310nm
5	280nm	350nm	15	300nm	300nm
6	270nm	340nm	16	280nm	340nm
7	280nm	300nm	17	310nm	280nm
8	310nm	320nm	18	310nm	270nm
9	310nm	290nm	19	260nm	320nm
10	310nm	320nm	20	370nm	240nm

For these optimal device parameters, an FDTD-analysis was performed to assess the optical bandwidth of the device. The spectral dependence of the grating to fiber coupling efficiency is plotted in Fig. 6(a). A 3dB optical bandwidth of 85nm is obtained. This is larger than the 60nm 3dB bandwidth obtained in the standard grating coupler structure [6] and is related to the higher refractive index contrast in the proposed grating coupler structure. A field plot of the optimized structure when the grating coupler is illuminated by the fiber optical mode at a wavelength of 1.55 μ m is plotted in Fig. 6(b).

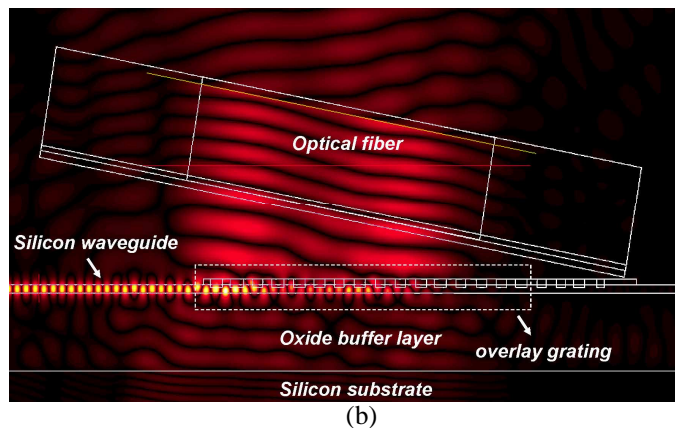
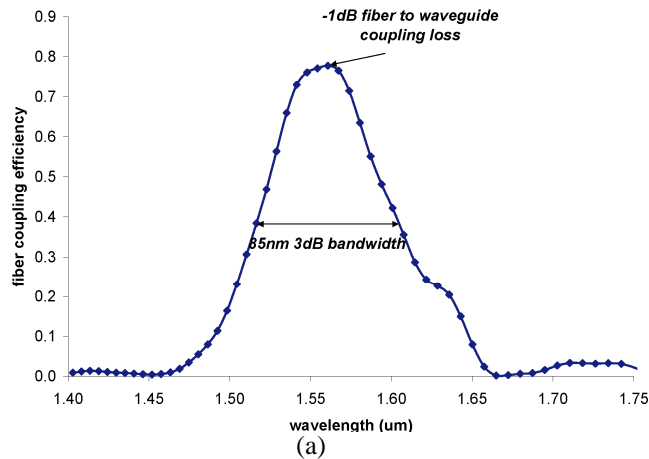


Fig. 6. Fiber coupling efficiency as a function of wavelength (a) and a field plot of the grating coupler structure excited by the TE optical fiber mode at a wavelength of 1.55 μm (b).

Although the diameter of the optical fiber cladding was decreased to reduce the FDTD simulation window, the presence of a 125 μm diameter fiber core (resulting in an increase of the fiber to grating separation) is not expected to impact the fiber coupling efficiency as the minimum obtainable separation of $62.5\mu\text{m} \times \tan(10^\circ) = 11\mu\text{m}$ is much smaller than the Rayleigh range (indicating the onset of substantial diffraction of a Gaussian beam) of $\pi w^2/\lambda = \pi(4.5\mu\text{m})^2/1.55\mu\text{m} = 41\mu\text{m}$ for a Gaussian beam with a waist radius of 4.5 μm , as is the case for a single mode optical fiber.

4. Tolerance analysis

In the fabrication of the grating coupler structure, deviations from the designed grating structure can occur. The thickness of the deposited poly-Silicon layer or the etch depth can vary. The position of the mask to define the grating can vary with respect to the edge of the deposited poly-Silicon overlay, which results in an uncertainty of the size of the first and last grating tooth. Also hard to predict variations of the individual grating teeth and slit width can occur due to proximity effects in the deep UV lithography of the grating structure. Finally, the position of the optical fiber can be different from the optimal position. The influence of the poly-Silicon layer thickness and the grating etch depth variation is plotted in Fig. 7. A +/- 10% deviation from the optimal device parameters is assumed. From these calculations it is

clear that this type of fabrication error predominantly results in a shift of the resonance wavelength of the grating coupler.

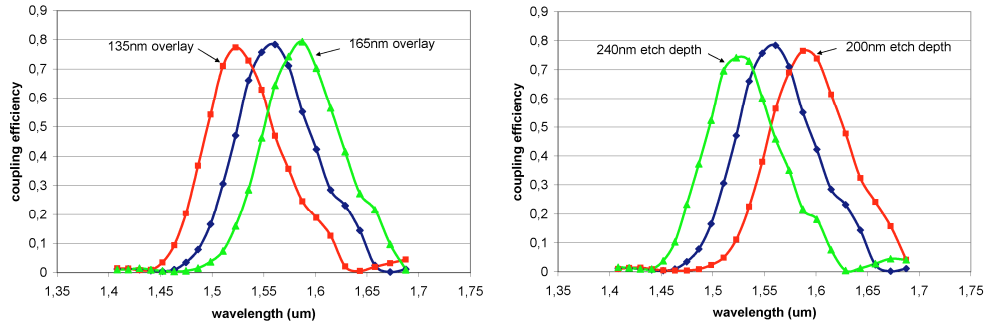


Fig. 7. Influence of the poly-Silicon overlay layer thickness (a) and the grating etch depth (b) on the fiber to waveguide grating coupler spectrum.

Although the misalignment between the grating etch mask and the poly-Silicon overlay mask results in an uncertainty of the size of the first and the last grating tooth, nearly all light has been diffracted from the waveguide when reaching the last tooth and therefore only the influence of the width of the first grating tooth is important. This influence is assessed in Fig. 8(a), showing that a $\pm 100\text{nm}$ alignment accuracy is sufficient for high device performance. This can easily be achieved using a standard CMOS stepper. In Fig. 8(b), the influence of random variations of the grating coupler parameters due to illumination proximity errors are shown. Random variations of $\pm 10\%$ on all grating tooth and slit widths were assumed.

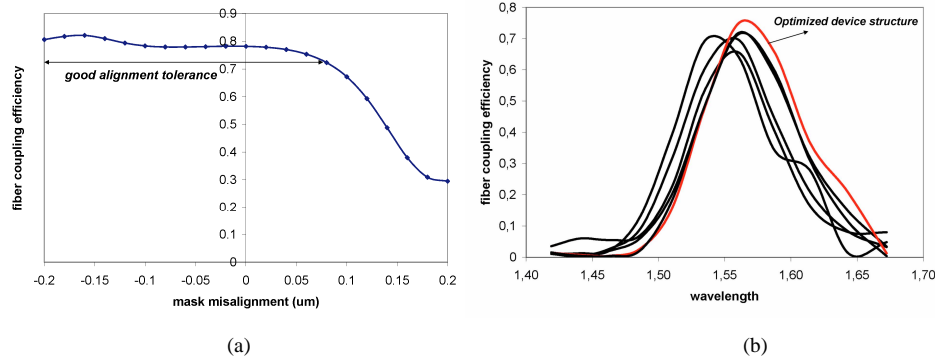


Fig. 8. Influence of the alignment between the poly-Silicon overlay and the grating etch mask on the coupling efficiency at $1.55\mu\text{m}$ – a negative mask misalignment results in a narrower first grating tooth - (a) and the influence of random variations of the grating coupler tooth and slit widths on the grating coupler spectrum (b).

Finally, the influence of the position of the optical fiber along the direction of propagation of the excited Silicon waveguide mode on the grating coupler efficiency was assessed. This is depicted in Fig. 9, showing a good alignment tolerance for the position of the optical fiber. A 1dB misalignment tolerance of $\pm 1.5\mu\text{m}$ is obtained.

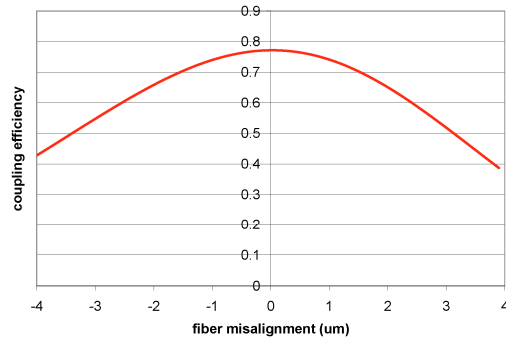


Fig. 9. Influence of the fiber position along the direction of propagation of the excited Silicon waveguide mode on the grating coupler efficiency.

5. Conclusions

In this paper, a new type of grating coupler structure was presented for high efficiency coupling between an SOI waveguide and a single mode optical fiber. The grating coupler structure consists of a poly-Silicon overlay in the grating region and a non-uniform etched grating, which can be fabricated using standard deep UV lithography. A fiber coupling efficiency of 78% with a 3dB optical bandwidth of 85nm is feasible using this type of device.

Acknowledgments

This work was partly supported by the Belgian IAP-PHOTON network, the IWT-SBO epSOC project and the Fund for Scientific Research (FWO Vlaanderen).